HHS Public Access

Author manuscript

Free Radic Biol Med. Author manuscript; available in PMC 2020 August 01.

Published in final edited form as:

Free Radic Biol Med. 2019 August 01; 139: 24–34. doi:10.1016/j.freeradbiomed.2019.05.015.

p66Shc Protein through a Redox Mechanism Enhances the Progression of Prostate Cancer Cells towards Castration-Resistance

Dannah R. Miller[1,°], **Matthew A. Ingersoll**[1,°,┼], **Arpita Chatterjee**[1], **Brian Baker**[2], **Shashank Shrishrimal**[1], **Elizabeth A. Kosmacek**[1], **Yuxiang Zhu**[1], **Pi-Wan Cheng**[1], **Rebecca E. Oberley-Deegan**[1], and **Ming-Fong Lin**[1,3,4,5,*]

[1]Department of Biochemistry and Molecular Biology, University of Nebraska Medical Center, Omaha, Nebraska, United States of America

[2]Department of Biology, Clark Atlanta University, Atlanta, GA, United States of America

[3]Section of Urology, Department of Surgery, University of Nebraska Medical Center, Omaha, Nebraska, United States of America

[4]Eppley Institute for Research in Cancer and Allied Diseases, University of Nebraska Medical Center, Omaha, Nebraska, United States of America

[5]College of Pharmacy, Kaohsiung Medical University, Kaohsiung, Taiwan

Abstract

Prostate cancer (PCa) remains the second leading cause of cancer-related deaths in U.S. men due to the development of the castration-resistant (CR) PCa phenotype. A useful cell model for analysis of the molecular mechanism of PCa progression is required for developing targeted therapies toward CR PCa. In this study, we established a PCa cell progressive model in three separate cell lines, of which androgen-independent (AI) cells were derived from respective androgen-sensitive (AS) cells. Those AI PCa cells obtain the biochemical properties of the clinical CR phenotype, including AR and PSA expression as well as enhanced proliferation and tumorigenicity under androgen-deprived conditions. Thus, those AI cells recapitulate CR PCa and exhibit increased oxidant species levels as well as enhanced signaling of proliferation and survival pathways. H_2O_2 treatment directly enhanced AS cell growth and migration, which was counteracted by antioxidant N-acetyl cysteine (NAC). We further identified p66Shc protein enhances the production of oxidant species which contributes to phenotypic and cell signaling

[*]**Corresponding Author:** Ming-Fong Lin, Ph. D, Department of Biochemistry and Molecular Biology, College of Medicine, University of Nebraska Medical Center, 985870 Nebraska Medical Center, Omaha, NE 68198-5870, USA, TEL: (402) 559-6658, FAX: (402) 559-6650, mlin@unmc.edu (MFL).

[°]These authors contributed equally to this manuscript

[┼]Current Address

Department of Pharmacology, Creighton University, Omaha, Nebraska, USA

Declaration of Interest

The authors declare no conflict of interest regarding the publication of this work.

alterations from AS to AI PCa cells. H_2O_2-treated LNCaP-AS cells had a similar signaling profile to that of LNCaP-AI or p66Shc subclone cells. Conversely, the oxidant species-driven alterations of LNCaP-AI and p66Shc subclone cell signaling is mitigated by p66Shc knockdown. Moreover, LNCaP-AI cells and p66Shc subclones, but not LNCaP-AS cells, develop xenograft tumors with metastatic nodules, correlating with p66Shc protein levels. Together, the data shows that p66Shc enhances oxidant species production that plays a role in promoting PCa progression to the CR stage.

Keywords

Prostate Cancer; p66Shc; ROS; Castration-Resistant Prostate Cancer

Introduction

Prostate cancer (PCa) is the most commonly diagnosed solid tumor and predicted to be the second leading cause of cancer-related deaths in 2019 for U.S. men [1]. Localized PCa is treated with surgery and radiation therapy, while the standard treatment for metastatic PCa is androgen deprivation therapy (ADT). Androgen receptor (AR) activation is vital for PCa survival and progression, therefore removal of its ligand, androgen, results in remission of the tumor. Unfortunately, there is a high likelihood of relapse and development of castration-resistant (CR) PCa, which is no longer responsive to ADT while AR remains functional. Desensitization to ADT can arise from multiple mechanisms such as intracellular biosynthesis of androgens, loss of AR fidelity, persistent activation of AR through mutation and alternatively spliced forms, or alternate pathways utilized to stimulate cell growth [2,3]. Currently, the treatment option for patients with CR PCa is limited, and several FDA-approved agents, such as docetaxel, can only extend the patient's life by only a few months [4]. Unfortunately, CR PCa patients will also quickly develop resistance to these drugs. Therefore, we investigated the molecular mechanism of CR PCa progression to identify novel target(s) for developing alternative therapies to treat this lethal disease.

Reactive oxygen species (ROS) play a vital role in mediating diverse cell signaling and apoptosis. ROS molecules are natural byproducts of cellular respiration and contribute to essential signaling pathways; local ROS production stimulated by external growth factors and hormones is an important source of signal transduction through the oxidation and reduction of proteins [5-9]. However, excess ROS, particularly free radicals, can also oxidize a number of vital molecules including DNA, lipids and proteins to promote cancer development [10-12]. Further, oxidant species such as H_2O_2 also regulates signaling pathways involved in diverse processes such as angiogenesis, cell adhesion, proliferation and migration, all of which are critical to cancer progression [12-15]. Results of several studies have shown that oxidation of protein tyrosine phosphatases via increased cellular oxidant species levels can inhibit its enzymatic activity; thus, leaving kinase activity unregulated, which results in promotion of cell proliferation and migration [9,16,17]. Cellular ROS has been proposed to regulate the progression of many types of cancers, including PCa [18]. For example, the protein levels of several NADPH oxidases (NOXs) increase upon progression to the CR phenotype in PCa tissues and cell lines [19-21]. Additionally, ROS has been

shown to promote PCa proliferation, migration, invasion and metastasis [9,21], and activation of AR can result in increased oxidant species due to augmented mitochondrial activity [9, 21-24]. While there are many studies on the correlative influence of ROS on PCa progression, the effects of ROS and its molecular mechanism by a specific oxidase/pro-oxidant protein with clinical relevance on PCa progression remains under investigation.

In this study, we reported the establishment of a PCa cell progression model including AR-positive LNCaP, MDA PCa2b and VCaP PCa cell lines, and investigated the role of oxidant species in androgen-sensitive (AS) and androgen-independent (AI) PCa tumorigenicity. In this progressive cell model, AI PCa cells exhibit many biochemical properties of CR phenotypes, including rapid proliferation and prostate-specific antigen (PSA) expression in steroid-reduced (SR) conditions as well as increased tumorigenicity and oxidant species levels. Interestingly, H_2O_2 treatment of AS cells increased cell growth and migration, which was counteracted by antioxidant N-acetyl-cysteine (NAC) treatment. Our studies revealed that in AI PCa cells, there were elevated protein levels of p66Shc, higher than that in the corresponding AS cells, as seen in clinical PCa archival specimens [9,25]. Elevated p66Shc protein leads to increased oxidant species levels via mitochondrial superoxide production and activation of NOX complexes via Rac1, which enhances activation of survival, growth and migration pathways [26,27]. Hence, our data clearly show the association between p66Shc protein and oxidant species levels in enhancing PCa tumorigenicity and promoting its progression. Importantly, LNCaP-AI cells and p66Shc subclones, but not LNCaP-AS cells, exhibited the metastatic ability upon orthotopic implantation in athymic mice, correlating with p66Shc protein levels. Together, our data show that elevated p66Shc protein via oxidant species production enhances AS PCa progression under androgen-deprived conditions and obtains the CR PCa phenotype, a lethal disease.

Materials and Methods

Materials

RPMI 1640 medium, DMEM medium, Keratinocyte SFM medium, gentamicin, and L-glutamine were obtained from Invitrogen (Carlsbad, CA, USA). HPC1 medium was purchased from Fischer Scientific (Pittsburgh, PA, USA). Fetal bovine serum (FBS) and charcoal-treated FBS were purchased from Atlanta Biologicals (Lawrenceville, GA, USA). Protein molecular weight standard markers, acrylamide, and Bradford protein assay kit were purchased from Bio-Rad (Hercules, CA, USA). Anti-CDC25B (#D2810, 1:1000), anti-cyclin B1 (#K1907, 1:1000), anti-cPSA (#E1812, 1:1000), anti-NFκB (#H052, 1:1000), anti-phospho-ErbB-2 (Y122/2) (#B2212, 1:1000), anti-ErbB-2 (#E3110, 1:1000), and horseradish peroxidase-conjugated anti-mouse (#C2011, 1:5000), anti-PAcP (#D0209, 1:1000), anti-PYK2 (#F061, 1:1000), anti-Rac1 (#G1905, 1:1000), anti-p42/p44 (#H1109, 1:1000), anti-Survivin (#C271, 1:1000), anti-PCNA (#G2G1, 1:1000), anti-Cyclin D1 (M-20, 1:1000), anti-rabbit (#D2910, 1:5000), anti-goat (#J0608, 1:5000) IgG antibodies (Abs) were all acquired from Santa Cruz Biotechnology (Santa Cruz, CA, USA). Anti-phospho-AKT (Ser473) (#GA160, 1:1000), anti-AKT (#C1411, 1:2000), anti-AR (#5153S, 1:3000), anti-phospho-p42/p44 (#9101S, 1:1000), anti-FOXM1 (#5436S, 1:500), anti-FOXO3a (#99199S, 1:500), anti-phospho-mTOR Ser2448 (#5536S, 1:1000), anti-mTOR

(#2972S, 1:1000), anti-Caspase 3 (9662S, 1:2000), anti-PARP (9532S, 1:2000), and anti-YAP1 (#4912, 1:1000) Abs were from Cell Signaling Technology (Beverly, MA, USA). Anti-GTP-Rac1 (#G052YWF2, 1:1000) Ab was obtained from New East Biosciences (Malvern, PA, USA). Anti-phospho-PYK2 Y402 (#CDRO0114121, 1:1000) and anti-Catalase (#AF3398, 1:2000) Abs were obtained from R&D Systems (Minneapolis, MN, USA). Anti-Shc (#06-203, 1:5000) and anti-p-Shc (#07-209, 1:1000) Ab was obtained from Upstate Biotech. Inc. (Lake Placid, NY, USA). Anti-Nrf2 (ab62352, 1:1000) and anti-phosphoYAP1 (Ser127) (ab52771, 1:1000) were purchased from Abcam. Anti-β-Actin (#99H4842, 1:10000) Ab, NAC, and H_2O_2 were purchased from Sigma (St. Louis, MO, USA).

Cell Culture

Human prostate cancer cell lines LNCaP, VCaP and MDA PCa2b were originally purchased from the American Type Culture Collection (Rockville, MD, USA) and cultured according to the accompanied protocols and our publications [28-32]. To mimic the conditions of clinical ADT, cells were maintained in SR conditions, i.e. phenol red-free RPMI 1640 medium containing 5% charcoal-stripped FBS, 2 mM glutamine, 50 μg/ml gentamicin and 1 nM 5α-dihydrotestosterone (DHT), for 2 days prior to experiments.

AI LNCaP C-81 cells were established according to our previous publications [28,29,33]. LNCaP C-81 cells exhibit biochemical properties similar to CR PCa, including proliferation and prostate-specific antigen (PSA) secretion in SR conditions, and importantly, obtaining intracrine regulation by synthesizing endogenous testosterone from cholesterol with activated AR [3]. Within this manuscript to be consistent with the other AI cells, LNCaP C-81 cells are abbreviated as LNCaP-AI cells. Similarly, we established MDA PCa2b-AI and VCaP-AI cells that obtained the AI phenotype, including AR expression and rapid cell proliferation [30-32].

Cell Proliferation

To determine PCa cell growth, AS and AI LNCaP, MDA PCa2b, and VCaP cells were plated at 2×10^4, 1×10^5, and 2×10^5 cells per well in 6-well plates, respectively, for three days. Cells were then adjusted to SR medium for 48 hours, as indicated. Cells were harvested every 72 hours for 9 days. The cell number was counted by a cell counter cellometer™ Auto T4 (Nexcelom Bioscience, USA) using Trypan blue dye exclusion assay [9,32-35].

Transwell Cell Migration Assay

The Boyden chamber transwell assay was utilized to determine the migratory ability of AS and AI PCa cells. AS and AI LNCaP, MDA PCa2b and VCaP cells were plated in the upper chamber of the 24-well insert at 5×10^4 cells per insert in regular medium. After 24 hours, cells were stained with 0.2% crystal violet containing 50% methanol. Migrated cells in the lower part of the chamber were counted at 40x magnification [30, 32-34].

Clonogenic Colony Formation Assay

For the clonogenic assay on a plastic surface, AS and AI LNCaP, MDA PCa2b and VCaP cells were plated in 6 well plates at 3,000, 10,000, and 10,000 cells per well, respectively, in

regular medium with a change of fresh medium every 72 hours. On day 9, cells were washed with HEPES-buffered saline and attached cells on the plastic surface were stained and fixed with 0.2% crystal violet containing 50% methanol. The stained cells were then photographed for counting [31,32,34,35].

General Oxidant Species Detection

To analyze cellular levels of general oxidant species, cells were stained with 20 μM DCF-DA in the dark for 30 minutes before being washed with PBS and analyzed via a Becton-Dickinson fluorescence-activated cell sorter (FACSCalibur, Becton Dickinson, San Jose, CA, USA) at the UNMC Flow Cytometry Core Facility [9,27,35,36,37]. Cells were also stained with PO-1 (1 mM) and MitoSOX (5 μM) to detect H_2O_2 and mitochondrial $O_2^{\bullet -}$, respectively. Briefly, cells were stained with the respective reagents for 1 hour and then fixed with 4% paraformaldehyde for 10 minutes [35]. DAPI was used for nuclear staining. Cells were visualized under a confocal microscope at 60x.

Transfection

For transient transfection experiments, LNCaP cells and p66Shc cDNA-transfected subclones were plated at a density of 1×10^4 cells per cm^2 and transfected using Lipofectamine and Plus reagents. Stable subclones of LNCaP cells that overexpress p66Shc via cDNA transfection were established as described previously [38]. For knock-down of p66Shc expression, transient transfection of pSUP-p66 plasmid-based small interfering RNA system targeted against the CH2 domain was used as described previously [27,38].

Phosphoprotein Microarray

For the phosphoprotein microarray, aliquots of cell lysates from LNCaP-AS and LNCaP-AI cells as well as an equal amount of mixed stable p66Shc cDNA-transfected subclones and V1 vector alone-transfected control cells were sent to Kinexus Protein Profiling Services (Vancouver, BC) where the company performed analysis via the KAM-900P microarray. Results are reported shown as increased (red) or decreased (green) fold-change of phosphoproteins in LNCaP-AI compared to LNCaP-AS cells or p66Shc subclones compared to V1 vector-alone transfected cells [27].

Immunoblot Analysis

For immunoblot analyses, cells were washed with HEPES buffered saline, pH 7.0, harvested by scraping, and lysed in ice-cold lysis buffer containing protease and phosphatase inhibitors. Protein concentrations of the supernatant were determined using Bio-Rad Bradford protein-assay. An aliquot of the total cell lysate was electrophoresed on SDS-polyacrylamide gels (7.5%-12%). After transfer to a nitrocellulose membrane, the membranes were blocked with 5% non-fat milk in Tris-buffered saline (TBS) containing 0.1% Tween-20 for 60 minutes at room temperature. Membranes were incubated with the corresponding primary Ab at 4°C overnight. Membranes were rinsed with TBS and incubated with the proper secondary Ab for 60 minutes at room temperature. Proteins were detected using enhanced chemiluminescence (ECL) reagent kit. β-actin was used as a loading control [27,32,34,35].

Implantation of tumor cells

For the orthotopic implantation, athymic mice were anesthetized by continuous flow of 2.5% isoflurane with oxygen using a mouse anesthesia machine. LNCaP-AS, LNCaP-AI, LNCaP-AI-Luc, V1 or p66Shc subclone cells (50 μl containing 2.0×10^6 cells in 50% Matrigel) were injected into the dorsal prostatic lobe using a 30-gauge needle. The peritoneal tissues were closed in two layers with absorbable catgut sutures (563B, Surgical Specialties, Tijuana, Mexico). Buprenorphine (0.1 mg/kg, Reckitt Benckiser Healthcare (UK) Ltd., Hull, England) was administrated by intraperitoneal route immediately after the surgery followed by three doses at six, twenty-four and forty-eight hours after surgery. Sterile surgical procedures were maintained for the entire process [38]. For subcutaneous tumor implantation, 1×10^6 cells (200 μl with 50% Matrigel) were injected into the dorsal surface of the mice via a 26-gauge needle [28,29]. All experimental procedures were approved by UNMC IUCAC (IUCAC #14-054-08FC) and carried out in accordance with institutional and federal guidelines.

Bio-luminescence imaging

LNCaP-AI-Luciferase-inoculated mice were imaged at three or five weeks after intraprostatic injection of cancer cells. For imaging, D-Luciferin potassium salt (100 mg/kg, PerkinElmer, #122799, Waltham, MA, USA) was dissolved in sterile PBS and injected intraperitoneally into the tumor bearing mice 15 minutes prior to imaging. For imaging the luciferase-expressing tumors, mice were anesthetized using 2.5% isoflurane with oxygen and placed in the Xenogen IVIS Spectrum bioluminescence imaging system (PerkinElmer, MA, USA). Images were acquired and analyzed by Living Image 4.5.1 software (Caliper Life Sciences, MA, USA) with an exposure time of one second. Regions of interest were determined to encompass the area with most intense light, and signal intensity was calculated based on a measurement of photons/s/cm^2/sr [39]. All experimental procedures were approved by UNMC IUCAC (IUCAC #07-087-12EP) and carried out in accordance with institutional and federal guidelines.

Statistical Analysis

Experiments were repeated independently at least three times with two or three technical replicates in each independent experiment as specified in each figure legend. For example, an experiment completed three times with two technical replicates in each experiment would be indicated by n=2×3. The average value of the technical replicates was utilized for each independent experiment, i.e., n=3, for statistical analysis. The mean and standard deviation values of results were calculated from the values obtained after three independent experiments and two-tailed student-t test via Microsoft excel was used to determine the significance of results. Equal variances were assumed for the two populations. $p<0.05$ was considered statistically significant. Quantification of western blot bands was performed on the NIH program Image-J before undergoing statistical analysis.

Results

Proliferation of AS and AI PCa Cells in Regular and SR Conditions

To demonstrate the AI phenotype, we analyzed the proliferation of AS PCa cells and the corresponding AI counterparts in both regular steroid-containing and SR conditions via Trypan blue exclusion assay. Proliferating Cell Nuclear Antigen (PCNA), a proliferative marker, was analyzed by Western blotting. In regular culture conditions that contain androgenic activity, LNCaP-AI, MDA PCa2b-AI and VCaP-AI cells have rapid growth rates, higher than the corresponding LNCaP-AS, MDA PCa2b-AS and VCaP-AS cells (Fig. 1A-C). Western blot analyses showed that AI cells have higher levels of PCNA compared to their AS counterparts. In SR conditions, the differential growth rates were even more pronounced because AS cells have dramatically reduced proliferative ability in androgen-deprived conditions, while AI cells retain their rapid growth rates (Fig. 1D-F). Nevertheless, it should be noted that while AI cells proliferate well in SR conditions, the growth rate is reduced compared to be in regular conditions. In summary, all three AI PCa cells proliferate rapidly in SR conditions.

Colony Formation and Migration of AS and AI PCa Cells

The tumorigenicity of AS and AI cells were analyzed by plastic surface 2-D clonogenic and Boyden chamber transwell assays. LNCaP-AI, MDA PCa2b-AI and VCaP-AI cells had increased ability of colony formation and migration, compared to their respective AS counterparts. LNCaP-AS cells formed an average of 50 colonies compared to 214 LNCaP-AI colonies (Fig. 2A). MDA PCa2b-AS and VCaP-AS cells grew 30 and 35 colonies, respectively, while their AI counterparts formed 338 and 172 colonies (Fig. 2B and 2C). In the Boyden chamber transwell assay, LNCaP-AI cells migrated approximately 2-fold after 24 hours compared to LNCaP-AS cells (Fig. 2D). MDA PCa2b-AI and VCaP-AI cells have migratory rates about 3-fold and 4-fold of the MDA PCa2b-AS and VCaP-AS cells, respectively (Fig. 2E and 2F). Thus, the tumorigenicity of AI cells increases, higher than the corresponding AS cells.

Basal Oxidant Species Levels and Cell Signaling Profiles in AS and AI PCa Cells

Because ROS levels have been proposed to play a role in PCa progression [18,21,22], we semiquantified the relative basal oxidant species levels in AS and AI PCa cells utilizing DCF-DA dye, which primarily measures H_2O_2 [37]. As shown in Fig. 3A, a significantly greater amount of fluorescence was detected in LNCaP-AI cells compared to LNCaP-AS cells (Fig. 3A). Similarly, MDA PCa2b-AI (Fig. 3B) and VCaP-AI (Fig. 3C) cells had significantly higher basal levels of general oxidant species compared to corresponding AS cells. On average, AI PCa cells had about 40% higher basal general oxidant species levels than their respective AS PCa cells.

Western blot analysis was conducted to analyze the signaling profiles of our PCa progressive cell model (Fig. 3D). Among three Shc family members, p66Shc protein level was elevated in LNCaP-AI, MDA PCa2b-AI and VCaP-AI cells compared to their AS counterparts; while the protein levels of the other two Shc isoforms, p52Shc and p46Shc, were not significantly altered in the respective AI cells. While AR protein levels showed only a minor change in

the three progressive cell lines, cellular PSA (cPSA), an androgen-regulated biomarker in PCa cells, was greatly elevated in AI PCa cells, indicating AR activation [33]. Cellular Prostatic Acid Phosphatase (cPAcP), a negative regulator of ErbB-2 phosphorylation and inhibitor of PCa growth [9, 38], was more readily reduced in LNCaP-AI and MDA PCa2b-AI cells, while there was only a minor change in VCaP-AI cells compared to VCaP-AS cells (the 50kDa protein is the active form of PAcP, while the 37 kDa protein is the intermediate form). Importantly, in all three AI PCa cells, there were increased phosphorylation levels of ErbB-2, AKT, ERK1/2 and mTOR compared to their AS counterparts. ROS-sensitive FOXM1 and its downstream CDC25B and Cyclin B1 were increased upon progression to the AI phenotype. There were also increased phosphorylation of PYK2 and elevated levels of P-Rex1 and GTP-bound Rac1, the activated form of Rac1, in AI PCa cells, both important proteins involved in cell migration. YAP1 phosphorylation and its total protein levels increased upon progression from AS to AI cells as well. In summary, the signaling profile in these three PCa cell progressive models demonstrates that AI PCa cells have greater potential for cell survival, proliferation and migration compared to corresponding AS PCa cells.

Effects of ROS by H_2O_2 and NAC on AS PCa Cell Proliferation and Migration

Because ROS levels and proliferative signaling are activated in advanced clinical PCa and general oxidant species levels are elevated in AI PCa cells compared to respective AS PCa cells (Fig. 3), we analyzed the direct effects of H_2O_2 and antioxidant NAC, a ROS scavenger, on AS PCa cell growth and migration. H_2O_2 treatment at physiological levels increased cell proliferation with 10 μM promoting the optimal growth of LNCaP-AS cells. Conversely, NAC treatment reduced the basal cell growth and reduced H_2O_2-stimulated cell proliferation (Fig. 4A). Since H_2O_2 (10 μM) treatment led to the optimal increase in cell proliferation of LNCaP-AS cells, this concentration was utilized for H_2O_2 treatments throughout the rest of the study.

H_2O_2 (10 μM) treatment increased MDA PCa2b-AS cell growth by about 80%, while NAC (10 mM) treatment reduced the basal cell proliferation by an average of 50% (Fig. 4B). The combination of NAC abolished the stimulatory effect of H_2O_2 treatment on cell proliferation of MDA PCa2b-AS cells (Fig. 4B). A similar trend was seen in VCaP-AS cells in which H_2O_2 treatment increased about 50% cell proliferation, while NAC treatment effectively reduced both basal and H_2O_2-stimulated cell proliferation (Fig. 4C).

H_2O_2 and NAC treatments exhibited similar respective effects on cell migration in all three AS cell lines observed in cell proliferation. H_2O_2 (10 μM) treatment increased cell migration by about 70%, 30%, and 50% in LNCaP-AS, MDA PCa2b-AS and VCaP-AS cells, respectively; NAC (10 mM) treatment reduced migration to below basal levels. Further, NAC reduced H_2O_2-enhanced migration by about 30-50% compared to control cells (Fig. 4D- 4F).

The effects of H_2O_2 and NAC treatments on cellular H_2O_2 levels was examined in LNCaP-AS cells as the model system. LNCaP-AS cells were stained with Peroxy Orange-1 (PO-1) to detect H_2O_2 levels. In LNCaP-AS cells, H_2O_2 (10 μM) treatment significantly increased H_2O_2 levels by about 50%, while NAC (10 mM) treatment resulted in a 20% reduction of

basal H_2O_2 levels. Concurrent treatment with H_2O_2 and NAC could effectively abolish the effects of H_2O_2 on the cellular oxidative environment (Fig. 4G). Thus, cellular levels of ROS/H_2O_2 correlate with H_2O_2 and NAC treatments resulting in altered cell proliferation and migration.

Cell Growth and Cellular Levels of Oxidant Species in LNCaP-AS and LNCaP-AI Cells and p66Shc Subclones

Because p66Shc protein levels are elevated in all three AI cells (Fig. 3D) and also clinical PCa [9,25], we determined the effect of p66Shc protein on cell growth (Fig. 5A and 5B) and analyzed H_2O_2 (DCF-DA and PO-1) and mitochondrial superoxide (MitoSOX) levels in LNCaP-AS and LNCaP-AI cells as well as p66Shc-overexpressing subclones versus V1 control cells. Comparing LNCaP-AI cells transfected with p66Shc shRNA to control cells, there was 60% reduction in cell proliferation (Fig. 5A). Upon stable transfection of LNCaP-AS cells with p66Shc cDNA, there was about 140% increase in cell proliferation compared to vector-alone V1 control cells, while there was a 60% reduction in cell proliferation in the stable p66Shc subclones upon knockdown of p66Shc protein (Fig. 5B).

To determine the role of p66Shc protein in enhancing oxidant species production, DCF-DA analysis was utilized upon knockdown of p66Shc. p66Shc knockdown in LNCaP-AI cells resulted in a 40% reduction in DCF-DA fluorescence (Fig. 5C). Comparing p66Shc subclones to V1 control cells, there was about a 35% increase in general oxidant species, as indicated by DCF-DA, while subsequent knockdown of p66Shc in these cells reduced DCF-DA fluorescence to basal V1 levels (Fig. 5D). As shown in Figure 5E, comparing the basal H_2O_2 levels in LNCaP-AS with LNCaP-AI cells, H_2O_2 levels are 50% greater in AI cells than AS cells and about 75% greater in p66Shc subclones compared to V1 control cells transfected with the vector alone. Importantly, transfection of LNCaP-AI cells or p66Shc subclones with p66Shc shRNA resulted in a decrease in PO-1 staining to that of basal levels seen in LNCaP-AS cells or V1 vector-alone transfected cells (Fig. 5E). Furthermore, MitoSOX fluorescence in LNCaP-AI cells was about 5-fold greater than in LNCaP-AS cells. Similarly, p66Shc subclones had an average of 3.5-fold greater mitochondrial superoxide levels compared to control cells transfected with the vector alone. Similar to PO-1 staining, upon transfection with p66Shc shRNA, MitoSOX fluorescence was reduced to that of LNCaP-AS or V1 cell levels in LNCaP-AI and p66Shc subclones (Fig. 5F). Therefore, increased p66Shc protein levels in both LNCaP-AI cells and p66Shc stable subclones are associated with a significant increase in H_2O_2 and mitochondrial $O_2^{\bullet -}$ levels, correlating with the AI phenotype.

Cell Signaling Profile in LNCaP Cells and p66Shc Subclones

To identify the common functional molecules in CR PCa progression, LNCaP and p66Shc subclone cell lysates under regular culture conditions were analyzed for alteration of phosphoproteins by Kinexus. Figure 6 shows that several functional proteins with elevated phosphorylation levels are consistent between LNCaP-AI cells and p66Shc subclones. For example, phosphorylation levels of ABL1, ACK1, AKT2, AKT3, AMPKα2, ANKRD3/RIPK4, APP, EGFR, ErbB2, ErbB3, MET and mTOR were elevated. Nevertheless, p66Shc subclones had an increase in phosphorylation of MAPKs including ERK2 and ERK5,

MKK2 and MEKK2, as well as activation of PKC and cyclin dependent kinases CDK1, CDK4, CDK10 and CDK12. Together, the data shows several signaling pathways, such as MET, ABL1 and the ErbB family, are activated in both LNCaP-AI cells and p66Shc subclones, suggesting that these pathways are altered upon progression to the AI phenotype with increased ROS levels.

Additionally, we performed molecular profiling on ROS-sensitive functional molecules by western blot analysis (Fig. 7) to validate and expand upon the phosphoprotein microarray. LNCaP-AS cells were treated with H_2O_2 (0-20 μM), NAC (10 mM), or a combination of H_2O_2 (10 μM) and NAC (10 mM) for 48 hours. While there was an apparent increase of p66Shc protein levels in AS cells upon treatment with H_2O_2, the protein level was still quite low. There were no significant changes in AR or cPSA protein levels. cPAcP protein levels were reduced upon H_2O_2, NAC, or the combination treatment. Further, cell proliferation and survival proteins ErbB-2, AKT, ERK and mTOR had elevated phosphorylation levels with increasing concentrations of H_2O_2, which was counteracted by NAC. FOXM1 protein levels as well as phosphorylated PYK2 and GTP-bound Rac1 increased with H_2O_2 treatment, while NAC treatment alone reduced activation of these proteins (Fig. 7A). Importantly, a similar signaling profile was seen in p66Shc subclones compared to vector-alone transfected V1 cells. p66Shc protein levels were increased in the p66Shc subclones as well as enhanced phosphorylation of ErbB-2, AKT, ERK, mTOR and PYK2 compared to V1 cells. FOXM1 levels were also increased in p66Shc subclones. Interestingly, cPAcP levels were reduced upon increased p66Shc expression (Fig. 7B). Further, knockdown of p66Shc in LNCaP-AI cells and stable p66Shc subclones resulted in reduced p66Shc and FOXM1 protein levels and decreased phosphorylation of ErbB-2, AKT, ERK, mTOR and PYK2. Conversely, cPAcP levels were increased, especially the 50 kDa form (Fig. 7B). The data demonstrates that these signaling pathways are sensitive to increased oxidant species and that p66Shc is one such source that could alter cell signaling in PCa.

LNCaP Progressive Cell Model and p66Shc Subclones in Xenograft Mouse Models

We determined the effect of p66Shc protein expression on *in vivo* tumorigenicity in xenograft animals. Initially, western blot analysis was utilized to determine protein levels of p66Shc in LNCaP-AS, LNCaP-AI, V1 and p66Shc subclone cells. Immunoblot analysis revealed that LNCaP-AS cells have the lowest levels of p66Shc, V1 and LNCaP-AI cells have moderate protein levels of p66Shc, and p66Shc subclones have the highest protein levels of p66Shc among the cell lines examined (Fig. 8A). To determine the *in vivo* tumor growth, these cells were subcutaneously injected into female athymic mice with low circulating androgens to mimic castrated conditions. Under castrated conditions in female mice, LNCaP-AS and V1 cells developed subcutaneous tumors in about 50% of the animals; while LNCaP-AI and p66Shc subclone cells developed tumors in at least 80% of the mice. LNCaP-AS and V1 tumors were in average about 193 mm^3 and 144 mm^3, respectively, while LNCaP-AI and p66Shc subclone tumors both had sizes of about 800 mm^3 (Fig. 8B). Thus, LNCaP-AI and p66Shc-overexpressing subclones obtain the enhanced tumorigenicity by developing more and larger tumors than AS cells in androgen-reduced environments, correlating with p66Shc protein levels.

To determine the effect of p66Shc expression on local invasion, LNCaP-AS and LNCaP-AI cells underwent orthotopic injection into the prostates of male athymic mice. As shown in Fig. 8B, no male mice developed metastatic tumors upon implantation with LNCaP-AS cells, while about 50% of mice with LNCaP-AI tumors exhibited metastasis. Additionally, 40% of mice with V1 tumors developed metastasis, while 100% of mice implanted with p66Shc subclone tumors developed metastasis (Fig. 8B). Collectively, p66Shc protein levels correlate with the metastatic frequency (Fig. 8A and 8B) with a linear correlation R-value of 0.8314. Figure. 8C clearly shows that orthotopic mouse models of LNCaP-AI-Luc cells develop metastatic tumors 3 weeks after implantation; while Figure 8D shows the metastasized tumors of p66Shc subclones in the pancreas and GI tract, which were the two most common metastasis locations (Fig 8E). Importantly, this data clearly demonstrates that the metastatic ability of PCa tumors correlates with p66Shc protein levels.

Discussion

CR PCa is a lethal disease that patients succumb to shortly upon development; thus, understanding the mechanism of PCa progression from the AS to the AI/CR phenotype is crucial for developing therapeutic options for this patient population. In this study, we report the establishment of a PCa cell progression model in three AR-positive PCa cell lines that recapitulates clinical PCa progression from the AS to the AI/CR phenotype. We further investigated the molecular mechanisms and determined that p66Shc protein/oxidant species play a vital role in PCa progression.

Results of Trypan blue exclusion, Boyden chamber transwell and clonogenic assays clearly show that all three AR-positive AI cells, including LNCaP-AI, MDA PCa2b-AI and VCaP-AI PCa cells, have greater tumorigenicity than respective AS cells, including proliferation, migration and colony formation (Fig. 1 and 2). Importantly, in SR conditions, AI PCa cells retained the rapid cell proliferation while the growth of AS PCa cells was arrested (Fig. 1). Further, AI PCa cells have higher levels of oxidant species including H_2O_2 than AS cells (Fig. 3A-3C), and AI cells have activated survival, proliferation and migration pathways (Fig. 3D). Significantly, activation of these pathways occur in clinical advanced PCa, such as AKT [40], ERK [41], mTOR [42], P-Rex1 [43-45] and YAP [46]. Increased P-Rex1 protein and Rac1 activity further suggest that AI PCa cells have greater migratory ability and potential for metastasis [47], as seen by the LNCaP-AI and p66Shc subclone xenograft tumors in Figure 8. It should also be noted that the early passages of V1 cells have similar low levels of p66Shc protein to LNCaP-AS cells [9, 38] and upon passage, the p66Shc protein levels increase similar to LNCaP-AI cells (Fig. 8A). Additionally, in PCa archival specimens, p66Shc protein level is elevated in PCa cancerous cells, higher than adjacent noncancerous prostate cells [9]. The data together supports the notion that p66Shc protein plays a role in supporting PCa progression and enhancing tumorigenicity and metastasis. Thus, we have established a useful PCa cell progression model in three AR-positive PCa cell lines that recapitulate clinical disease progression.

We also investigated the role of ROS in PCa progression. Interestingly, H_2O_2 treatments increased AS PCa cell proliferation and migration, which was competitively counteracted by NAC treatment (Fig. 4). We further analyzed p66Shc molecule that is shown to enhance

oxidant species generation for its role and mechanism involved in the phenotypic alteration from AS to AI/CR PCa cells [9,27,36,38]. LNCaP-AI cells and stable p66Shc-overexpressing subclones, which both exhibit the AI phenotype [9], had higher oxidative environments compared to LNCaP-AS and V1 cells (Fig. 5). Interestingly, the increase in $O_2^{\bullet-}$ is greater within the mitochondria, where p66Shc protein is often localized [36,48], further suggesting the role of p66Shc and mitochondrial $O_2^{\bullet-}$ generation in the AI PCa phenotype. Upon knockdown of p66Shc protein in LNCaP-AI and p66Shc subclone cells, there was a subsequent reduction in both ROS and oxidant species, as detected by DCF-DA, PO-1 and MitoSOX (Fig. 5). Analysis of ROS and $O_2^{\bullet-}$ levels with DHE resulted in a similar phenomenon in which both were reduced upon p66Shc knockdown (data not shown). Thus, our data clearly showed that p66Shc functions as a prooxidant to enhance oxidant species production which can promote PCa proliferation and progression.

To elucidate the molecular signaling mechanism of AI PCa cells, we performed a phosphoprotein microarray. Significantly, several proteins, including ABL1, AKT, ErbB-1/2/3, MET and mTOR, have enhanced activation in both LNCaP-AI cells and p66Shc subclones (Fig. 6). Our data further demonstrated oxidant species-mediated alterations in cell signaling profile with treatment of LNCaP-AS cells with H_2O_2 (Fig. 7), which was essentially identical to the AI PCa signaling profile in Figure 3D and validated increased phosphorylation levels of ErbB-2, AKT, ERK1/2 and mTOR seen in the phosphoprotein microarray results. Treatment of LNCaP-AS cells with H_2O_2 led to activation via increased phosphorylation of ErbB-2, AKT, ERK, mTOR and PYK2 as well as GTP-bound Rac1. We further confirmed that p66Shc expression affects the activation by phosphorylation of ErbB-2, AKT, ERK, mTOR and PYK2 in p66Shc subclones and by knockdown of p66Shc expression (Fig. 7B). Interestingly, many of these oxidant species-sensitive proteins are involved in cell survival, proliferation and migration such as MET, AKT [49], mTOR [50], ACK1 [51] and ABL1 [52]. Lastly, we demonstrated the ability of LNCaP-AI cells and p66Shc subclones, but not LNCaP-AS cells, to develop xenograft tumors in castrated conditions. Further, LNCaP-AI cells and p66Shc subclones exhibit enhanced metastatic ability, which correlates with p66Shc protein expression (Fig. 8). Supportively, p66Shc is shown to be elevated in clinical PCa archival specimens, suggestive of its vital role in enhancing PCa tumorigenicity and progression [9,25]. Our data together supports the notion that p66Shc could serve as a functional target and novel small molecule inhibitors to p66Shc should be developed for treatment of CR PCa.

Figure 9 represents the working hypothesis for the role of ROS in PCa progression. Suboptimal oxidant species levels can result in cell senescence, while a moderate increase in oxidant species levels promotes an environment in which cells exhibit the highest potential of proliferation, migration and invasion. AS PCa cells, including LNCaP-AS, MDA PCa2b-AS and VCaP-AS PCa cells, can increase protein levels of proteins that can promote ROS generation, such as p66Shc, or be treated with H_2O_2 to promote their tumorigenic phenotypes, while NAC or antioxidant enzymes will reduce cell growth (Fig. 9A). Moreover, increased oxidant species production via p66Shc protein can inactivate cPAcP, a prostate-specific, PTEN functional-homologue phosphatase [9], resulting in increased activity of ErbB-2, AKT, ERK, mTOR, PYK2 and Rac1, promoting PCa proliferation and survival (Fig. 9B).

Acknowledgements

We thank Dr. Jixin Dong for providing YAP and phospho-YAP1 antibodies, and Dr. Yaping Tu for the P-Rex1 antibody.

Funding

This study was supported in part by awards of the National Institutes of Health [CA88184, CA178888], the US Department of Defense PCRP Grants [PC121645 and PC141559], the University of Nebraska Food for Health Grant, the University of Nebraska Medical Center Advanced Microscopy Core Facility Grant, the Fred and Pamela Buffet Cancer Center Support Grant [P30CA036727], the UNMC Bridge Fund, the UNMC Buffet Cancer Center Pilot Project, the UNMC Cancer Biology Training Grant [T32CA009476], the UNMC Graduate Student Fellowship, and the Purdue Pharma Scholars Award at UNMC.

Abbreviations

Ab	Antibody
ADT	Androgen deprivation therapy
AR	Androgen Receptor
AS	Androgen-Sensitive
AI	Androgen-Independent
CR	Castration-Resistant
DHT	5α-Dihydrotestosterone
ECL	Enhanced chemiluminescence
FBS	Fetal Bovine Serum
H_2O_2	Hydrogen Peroxide
NOXs	NADPH Oxidases
NAC	N-acetyl-cysteine
PCa	Prostate Cancer
cPAcP	Celluar Prostatic Acid Phosphatase
PO-1	Peroxy Orange-1
PCNA	Proliferating Cell Nuclear Antigen
cPSA	Cellular Prostate-specific Antigen
ROS	Reactive Oxygen Species
$O_2^{\bullet-}$	Superoxide
SOD	Superoxide dismutase
SR	Steroid-reduced

TBS	Tris-buffered saline

References

1. Siegel RL, Miller KD, Jemal A. Cancer Statistics, 2019. CA: A Cancer Journal for Clinicians 2019 68(1): 7–34.
2. Seruga B, Ocana A, Tannock IF. Drug resistance in metastatic castration-resistant prostate cancer. Nat Rev Clin Onc 2012 8: 12–23.
3. Dillard PR, Lin MF, Khan SA. Androgen-independent prostate cancer cells acquire the complete steroidogenic potential of synthesizing testosterone from cholesterol. Mol Cell Endocrin 2008 295: 115–120.
4. Tannock IF, de Wit R, Berry WR, Horti J, Pluzanska A, Chi KN, et al. Docetaxel plus prednisone or mitoxantrone plus prednisone for advanced prostate cancer. N Engl J Med 2004 351: 1502–1512. [PubMed: 15470213]
5. Sauer H, Wartenberg M, Hescheler J. Reactive oxygen species as intracellular messengers during cell growth and differentiation. Cell Physiol Biochem 2001 11: 173–186. [PubMed: 11509825]
6. Levine RL. Carbonyl modified proteins in cellular regulation, aging, and disease. Free Radic Biol Med 2002 32(9): 790–796. [PubMed: 11978480]
7. Squier TC, Bigelow DJ. Protein oxidation and age-dependent alterations in calcium homeostasis. Front Biosci 2000 5: D504–526. [PubMed: 10799358]
8. Liou GY, Storz P. Reactive oxygen species in cancer. Free Radic Res 2010 44(5): 479–496. [PubMed: 20370557]
9. Veeramani S, Chou YW, Lin FC, Muniyan S, Lin FF, Kumar S, et al. Reactive oxygen species induced by p66Shc longevity protein mediate nongenomic androgen action via tyrosine phosphorylation signaling to enhance tumorigenicity of prostate cancer cells. Free Radic. Biol. Med 2012 53: 95–108. [PubMed: 22561705]
10. Wiseman H, Halliwell B. Damage to DNA by reactive oxygen and nitrogen species: role in inflammatory disease and progression to cancer. Biochem J 1996 313: 17–29. [PubMed: 8546679]
11. North JA, Spector AA, Buettner GR. Cell fatty acid composition affects free radical formation during lipid peroxidation. Am J Physiol 1994 267: C177–188. [PubMed: 8048478]
12. Storz P Reactive oxygen species in tumor progression. Front Biosci 2005 10: 1881–1896. [PubMed: 15769673]
13. Kundu N, Zhang S, Fulton AM. Sublethal oxidative stress inhibits tumor cell adhesion and enhances experimental metastasis of murine mammary carcinoma. Clin Exp Metastasis 1995 13(1): 16–22. [PubMed: 7820952]
14. Brown NS, Bicknell R. Hypoxia and oxidative stress in breast cancer. Oxidative stress: its effects on the growth, metastatic potential and response to therapy of breast cancer. Breast Cancer Res 2001 3(5): 323–327. [PubMed: 11597322]
15. Burdon RH, Gill V, Rice-Evans C. Oxidative stress and tumour cell proliferation. Free Radic Res Commun 1990 11(1–3), 65–76. [PubMed: 1963620]
16. Meng TC, Fukada T, Tonks NK. Reversible oxidation and inactivation of protein tyrosine phosphatases in vivo. Mol Cell 2002 9(2): 387–399. [PubMed: 11864611]
17. Lee SR, Yang KS, Kwon J, Lee C, Jeong W, Rhee SG. Reversible inactivation of the tumor suppressor PTEN by H2O2. J Biol Chem 2005 277(23): 20336–20342.
18. Kruk J, Aboul-Enein HY. Reactive oxygen and nitrogen species in carcinogenesis: implications of oxidative stress on the progression and development of several cancer types. Mini Rev. Med. Chem 2017 17(11): 904–919. [PubMed: 28245782]
19. Oh B, Figtree G, Costa D, Eade T, Hruby G, Lim S, et al. Oxidative stress in prostate cancer patients: a systematic review of case control studies. Prostate Int. 2016 4(3): 71–87. [PubMed: 27689064]
20. Roy K, Wu Y, Meitzler JL, Juhasz A, Liu H, Jiang G, et al. NADPH oxidases and cancer. Clin. Sci (Lond.) 2015 128(12): 863–875. [PubMed: 25818486]

21. Kumar B, Sweaty K, Khandrika L, Meacham RB, Koul HK. Oxidative stress is inherent in prostate cancer cells and is required for aggressive phenotype. Cancer Res 2008 68(6): 1777–1785. [PubMed: 18339858]
22. Khandrika L, Kumar B, Koul S, Maroni P, Koul HK. Role of oxidative stress in prostate cancer. Cancer Lett. 2009 282(2): 125–136. [PubMed: 19185987]
23. Ripple MO, Henry WF, Rago RP, Wilding G. Prooxidant-antioxidant shift induced by androgen treatment of human prostate carcinoma cells. J Natl Cancer Inst 1997 89(1), 40–48. [PubMed: 8978405]
24. Kumar S, Kumar S, Rajendran M, Alam SM, Lin FF, Cheng PW, et al. Steroids upregulate p66Shc longevity protein in growth regulation by inhibiting its ubiquitination. PLoS One 2011 6(1): e5942.
25. Lee MS, Igawa T, Chen SJ, Van Bemmel D, Lin JS, Lin FF, et al. p66Shc protein is upregulated by steroid hormones in hormone-sensitive cancer cells and in primary prostate carcinomas. Int J Cancer 2004 108: 672–678. [PubMed: 14696093]
26. Galimov ER. The role of p66Shc in oxidative stress and apoptosis. Acta Naturae 2010 2(4): 44–51. [PubMed: 22649663]
27. Ingersoll MA, Chou YW, Lin JS, Yuan TC, Miller DR, Xie Y, et al. p66Shc regulates migration of castration-resistant prostate cancer cells. Cell Signaling 2018 46, 1–14.
28. Lin MF, Lee MS, Zhou XW, Andressen JC, Meng TC, Johansson SL, et al. Decreased expression of cellular prostatic acid phosphatase increases tumorigenicity of human prostate cancer cells. J Urol 2001 166: 1943–1950. [PubMed: 11586265]
29. Igawa T, Lin FF, Lee MS, Karan D, Batra SK, Lin MF. Establishment and characterization of androgen-independent human prostate cancer LNCaP cell model. Prostate 2002 50: 222–235. [PubMed: 11870800]
30. Yuan TC, Veeramani S, Lin FF, Kondrikou D, Zelivianski S, Igawa T, et al. ErbB-2 via PYK2 upregulates the adhesive ability of androgen receptor-positive human prostate cancer cells. Oncogene 2007 26: 7552–7559. [PubMed: 17563746]
31. Chen SJ, Karan D, Johansson SL, Lin FF, Zeckser J, Singh AP, et al. Prostate-derived factor as a paracrine and autocrine factor for the proliferation of androgen receptor-positive humane prostate cancer cells. The Prostate 2007 67: 557–571. [PubMed: 17221842]
32. Miller DR, Ingersoll MA, Chou YW, Wakefield CB, Tu Y, Lin FF, et al. Anti-androgen abiraterone acetate improves the therapeutic efficacy of statins on castration-resistant prostate cancer cells. J Oncol Res Ther 2017 3: JONT-139.
33. Lin MF, Meng TC, Rao PS, Chang C, Schonthal AH, Lin FF. Expression of human prostatic acid phosphatase correlates with androgen-stimulated cell proliferation in prostate cancer cell lines. J Biol Chem 1998 273: 5939–5947. [PubMed: 9488733]
34. Ingersoll MA, Miller DR, Martinez O, Wakefield CB, Hsieh KC, Simha MV, et al. Statin derivatives as therapeutic agent for castration-resistant prostate cancer. Cancer Lett 2016 383(1): 94–105. [PubMed: 27687622]
35. Miller DM, Tzeng CC, Farmer T, Keller ET, Caplan S, Chen YS, et al. Novel CIL-102 derivatives as potential therapeutic agents for docetaxel-resistant prostate cancer. Cancer Lett 2018 436: 96–108. [PubMed: 30077739]
36. Veeramani S, Yuan TC, Lin FF, Lin MF. Mitochondrial redox signaling by p66Shc is involved in regulating androgenic growth stimulation of human prostate cancer cells. Oncogene 2008 27: 5057–5068. [PubMed: 18504439]
37. Kalyanaraman B, Darley-Usmar V, Davies KJA, Dennery PA, Forman HJ, Grisham MB, et al. Measuring reactive oxygen species and nitrogen species with fluorescent probes: challenges and limitations. Free Radic Biol Med 2012 52(1): 1–6. [PubMed: 22027063]
38. Veeramani S, Igawa T, Yuan TC, Lin FF, Lee MS, Lin JS, et al. Expression of p66Shc protein correlates with proliferation of human prostate cancer cells. Oncogene 2005 24: 7203–7212. [PubMed: 16170380]
39. Chatterjee A, Zhu Y, Kosmacek EA, Lichter EZ, Oberley-Deegan RE. The addition of manganese porphyrins during radiation inhibits prostate cancer growth and simultaneously protects normal prostate tissue from radiation damage. Antioxidants (Basel) 2018 7(1): 21.

40. Malik SN, Brattain M, Ghosh PM, Troyer DA, Prihoda T, Bedolla R, et al. Immunohistochemical demonstration of phospho-Akt in high gleason grade prostate cancer. Clin. Cancer Res 2002 8(4): 1168–1171. [PubMed: 11948129]
41. Price DT, Della Rocca G, Guo C, Ballo MS, Schwinn DA, Luttrell LM. Activation of extracellular signal-regulated kinase in human prostate cancer. J Urol 1999 162(4): 1537–1542. [PubMed: 10492251]
42. Kremer CL, Klein RR, Mendelson J, Browne W, Samadzedeh LK, Vanpatten K, et al. Expression of mTOR signaling pathway markers in prostate cancer progression. The Prostate 2006 66: 1203–1212. [PubMed: 16652388]
43. Wong CY, Wuriyanghan H, Xie Y, Lin MF, Abel PW, Tu Y. Epigenetic regulation of phosphatidylinositol 3,4,5-triphosphate-dependent Rac exchanger 1 gene expression in prostate cancer cells. J Biol Chem 2011 286(29): 25813–25822. [PubMed: 21636851]
44. Welch HC, Coadwell WJ, Ellson CD, Ferguson GJ, Andrews SR, Erdjument-Bromage H, et al. P-Rex1, a Ptdlns (3,4,5)P3- and Gbetagamma-regulated guanine-nucleotide exchange factor for Rac. Cell 2002 108(6): 809–821. [PubMed: 11955434]
45. Hernandez-Negrete I, Carretero-Ortega J, Rosenfeldt H, Hernandez-Garcia R, Calderon-Salinas JV, Reyes-Cruz G, et al. P-Rex1 links mammalian target of rapamycin signaling to Rac activation and cell migration. J Biol Chem 2007 282: 23708–23715. [PubMed: 17565979]
46. Jiang N, Hjorth-Jensen K, Hekmat O, Iglesias-Gato D, Kruse T, Wang C, et al. In vivo quantitative phosphoproteomic profiling identifies novel regulators of castration-resistant prostate cancer growth. Oncogene 2015 34: 2764–2776. [PubMed: 25065596]
47. Qin J, Xie Y, Wang B, Hoshino M, Wolff DW, Zhao J, et al. Upregulation of PIP3-dependent Rac exchanger 1 (P-Rex1) promotes prostate cancer metastasis. Oncogene 2009 28(16): 1853–1863. [PubMed: 19305425]
48. Giorgio M, Migliaccio E, Orsini F, Paolucci D, Moroni M, Contursi C, et al. Electron transfer between cytochrome c and p66Shc generates reactive oxygen species that trigger mitochondrial apoptosis. Cell 2005 122: 221–233 [PubMed: 16051147]
49. Organ SL. An overview of the c-MET signaling pathway. Ther Adv Med Oncol 2011 3: S7–S19. [PubMed: 22128289]
50. Acosta-Jaquez HA, Keller JA, Foster KG, Ekim B, Soliman GA, Feener EP, et al. Site-specific mTOR phosphorylation promotes mTORC1-mediated signaling and cell growth. Mol. Cell Biol 2009 29(15): 4308–4324. [PubMed: 19487463]
51. Mahajan K, Mahajan NP ACK1 tyrosine kinase: targeted inhibition to block cancer cell proliferation. Cancer Lett 2013 338(2): 185–192. [PubMed: 23597703]
52. Wang J, Pendergast AM. The emerging role of ABL kinases in solid tumors. Trends in Cancer 2015 1(2): 110–123. [PubMed: 26645050]

Highlights

- Prostate cancer cell progression model mimics clinical progression of castration-resistant cancer.
- Androgen-independent cells have a higher level of oxidant species than androgen-sensitive cells.
- Treatment of androgen-sensitive cells with hydrogen peroxide promotes growth and migration.
- p66Shc protein enhances oxidant species production with a castration-resistant signaling profile.
- p66Shc protein levels correlate with prostate cancer metastasis in xenograft animal model.

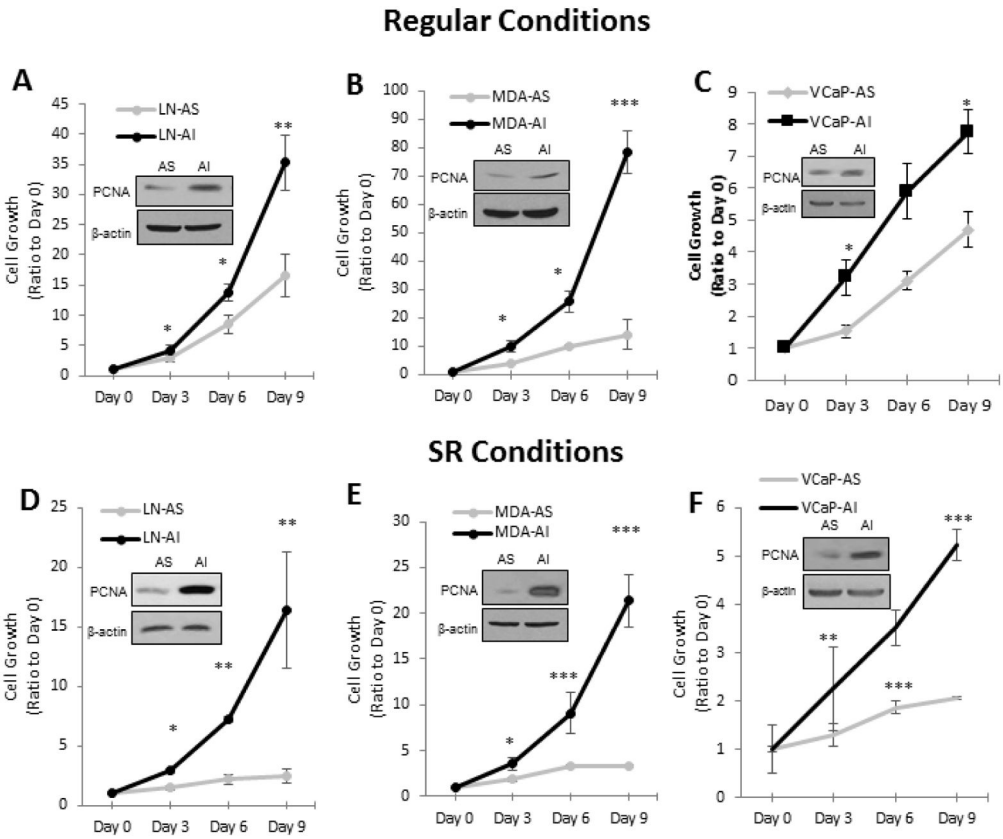

Figure 1. AS and AI PCa Cell Growth in Regular and SR Conditions.

AS and AI LNCaP, MDA PCa2b, and VCaP cells were subjected to a kinetic growth assay in (A-C) regular and (D-F) SR conditions. (A and D) LNCaP, (B and E) MDA PCa2b, and (C and F) VCaP cells were plated at 2×10^4, 1×10^5, and 2×10^5 cells per well in 6-well plates, respectively. For SR conditions, cells were adjusted to SR medium for 48 hours before growth determination. Cells were harvested every 72 hours on days 0, 3, 6, and 9. Cell viability was measured using Trypan blue exclusion dye. Results presented are mean ± SD. n=3×3. *p<0.05, **p<0.005, ***p<0.0005. Cells were lysed to determine PCNA levels via western blot analysis to confirm cell growth results. β-actin protein level was used as a loading control.

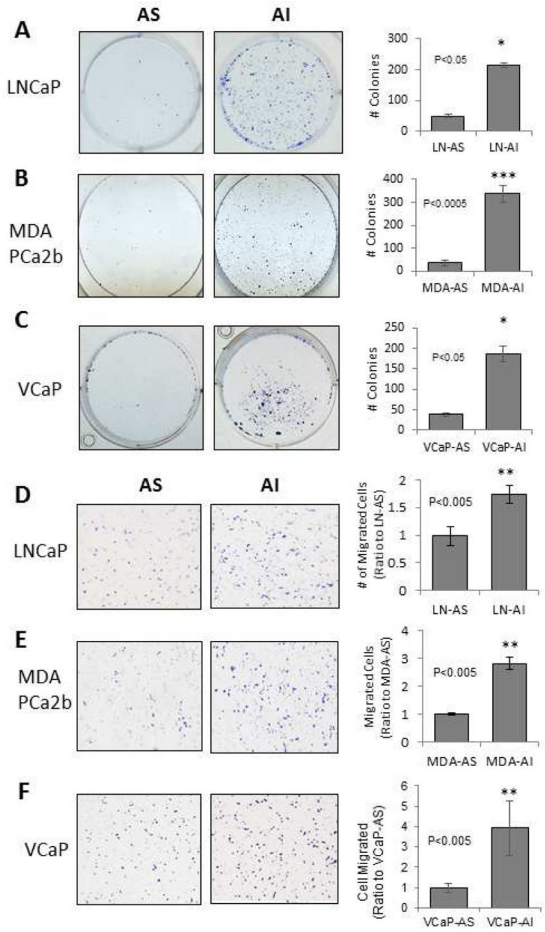

Figure 2. Colony Formation and Transwell Migration of AS and AI PCa Cells.

(A-C) AS and AI LNCaP, MDA PCa2b and VCaP cells were plated in 6-well plates at 3×10^3, 1×10^4 and 1×10^4 cells per well, respectively. LNCaP cells were maintained in regular RPMI 1640 medium for 9 days with a fresh change of medium every 3 days. MDA PCa2b and VCaP cell lines were maintained in HPC1 and DMEM, respectively, for 14 days, with a fresh change of medium every 3 days. Cells were stained with 0.02% crystal violet containing 50% methanol. The stained cells were then photographed at 40x magnification for counting. Results presented are mean ± SD. n=2×3. *p<0.05, **p<0.005, ***p<0.0005. (D-F) AS and AI LNCaP, MDA PCa2b and VCaP cells were plated in the upper chamber of the transwell inserts at 5×10^4, 6×10^4 and 6×10^4 cells, respectively, in regular medium. Cells were allowed to migrate for 24 hours, at which time cells in the upper chamber were removed via cotton swab and the cells that had migrated through the insert were stained with 0.02% crystal violet containing 50% methanol. Images were taken at 400x magnification. Results presented are mean ± SD. n=2×3. *p<0.05, **p<0.005.

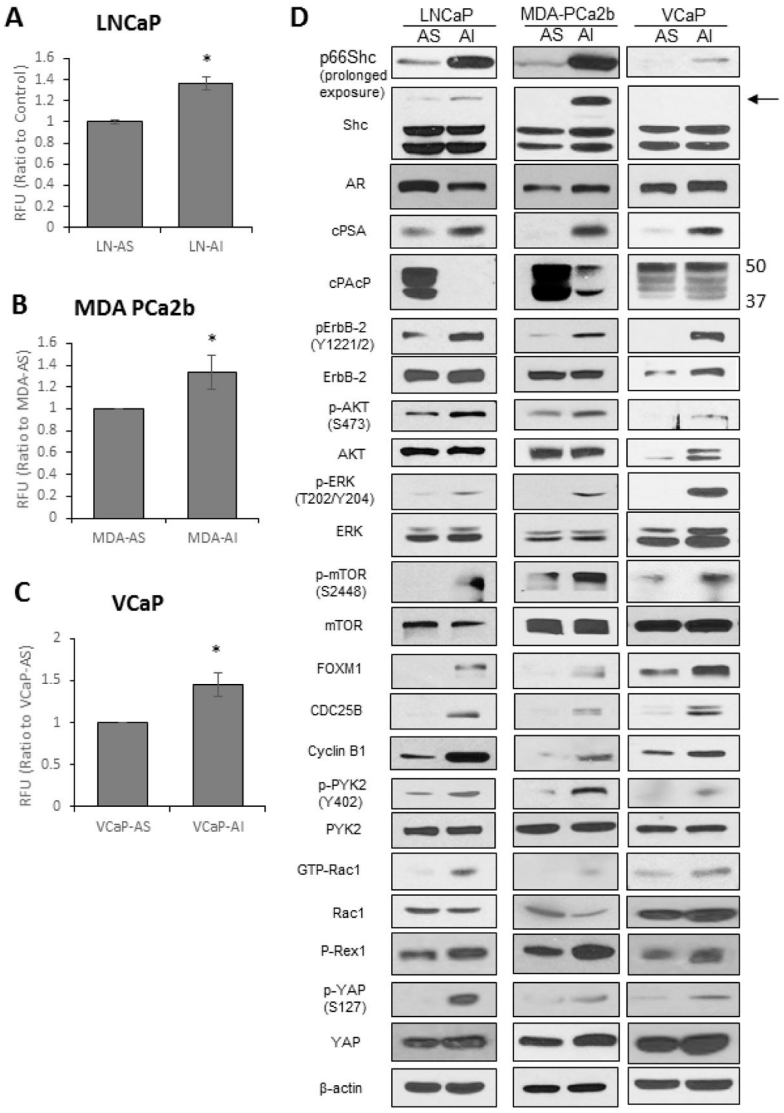

Figure 3. ROS Levels and Signaling Pathways in AS and AI Cells.

(A-C) DCF-DA analysis for general oxidant species levels. AS and AI (A) LNCaP, (B) MDA PCa2b and (C) VCaP cells were plated at 1×10^5, 5×10^5, and 3×10^5 cells per T25 flask and grown for 72 hours. Cells were stained with DCF-DA (20 μM) for 30 minutes in the dark and subjected to flow cytometry analysis. Results presented are mean ± SD. n=3, *$p<0.05$.

(D) Immunoblot analysis of the signaling pathways in LNCaP, MDA PCa2b and VCaP PCa cells. LNCaP, MDA PCa2b and VCaP cells were plated in T75 flasks at 1.5×10^4, 4×10^5 and 4×10^5 cells per flask in regular steroid-containing medium for 72 hours. Cells were harvested via scrapping and lysed. Total cell lysates were analyzed for Shc, AR, cPSA, PAcP, FOXM1, CDC25B, and Cyclin B1. Lysates were also analyzed for total and phosphorylated ErbB-2, AKT, ERK, mTOR, YAP1 and PYK2, as well as total Rac1 and GTP-Rac1. β-actin protein level was used as a loading control. The data shown is a

representative of three sets of independent experiments and similar results were obtained. n=3.

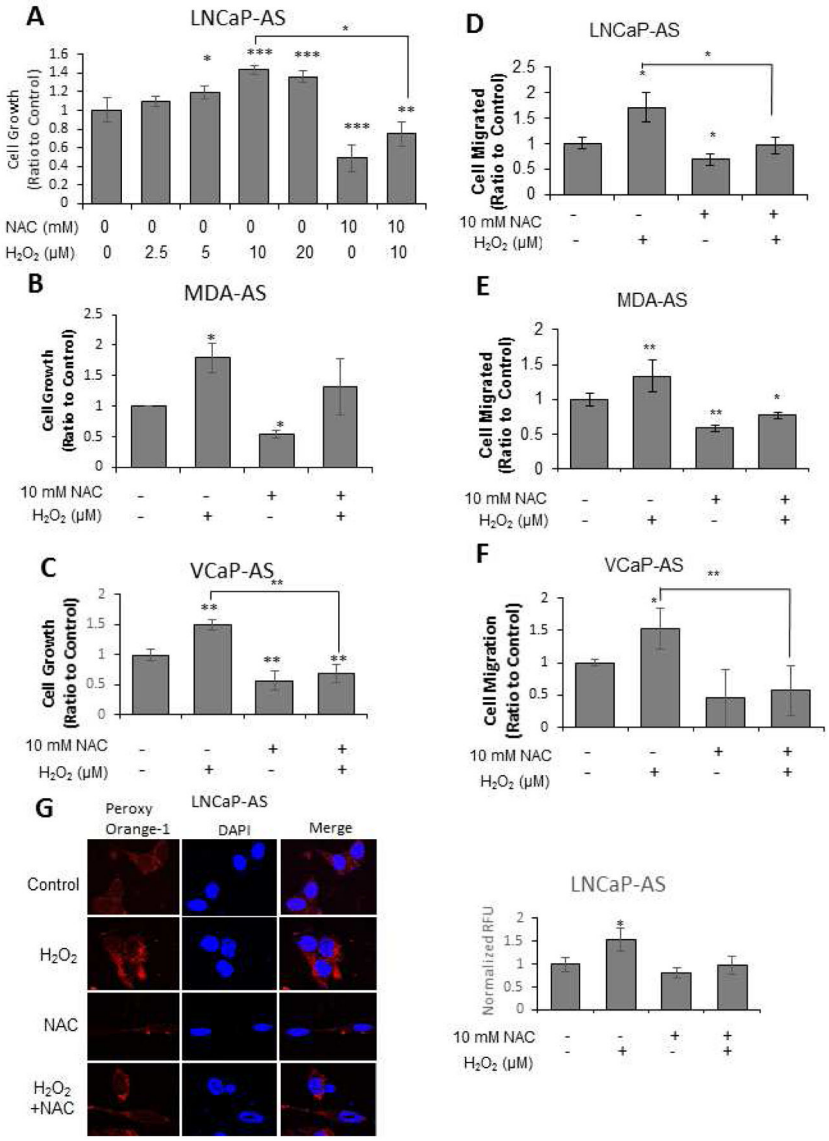

Figure 4. Effects of Altered Oxidant Species Levels on AS PCa Growth and Migration.

(A-C) Trypan Blue Exclusion Assay. (A) LNCaP-AS, (B) MDA PCa2b-AS and (C) VCaP-AS cells were plated at 2×10^4, 2×10^4 and 2×10^4 cells per well, respectively, for 72 hours. Cells were treated with H_2O_2 (0-20 μM) or NAC (10 mM) for 72 hours before cells were harvested and counted via Trypan blue exclusion dye. Results presented are mean ± SD. n=3×3. *p<0.05, **p<0.005, ***p<0.0005.

(D-F) Boyden Chamber Transwell Assay. (D) LNCaP-AS, (E) MDA PCa2b-AS and (F) VCaP-AS cells were plated at 5×10^4, 6×10^4 and 6×10^4 cells, respectively, in the upper chamber of a transwell insert for 24 hours with H_2O_2 (10 μM) and/or NAC (10 mM) treatments. Cells in the upper chamber were removed via cotton swab and the cells that had migrated through the insert were stained with 0.02% crystal violet containing 50% methanol. Images were taken at 400x magnification. Results presented are mean ± SD. n=2×3. *p<0.05, **p<0.005, ***p<0.0005.

(G) LNCaP-AS cells were plated at 5×10^4 cells per well in 12-well plates for 48 hours. Cells were treated with H_2O_2 (10 μM) and/or NAC (10 mM) for 24 hours. H_2O_2 levels were labeled with Peroxy Orange-1 fluorescence indicator for 1 hour before the reaction was quenched. DAPI was utilized to stain the nucleus. Fluorescence was visualized via a confocal microscope. Color adjustment was applied equally in all images shown. The data shown is a representative of three sets of independent experiments upon which 20 cells were quantified and similar results were obtained. Results presented are mean ± SD. n=3. *p<0.05, **p<0.005.

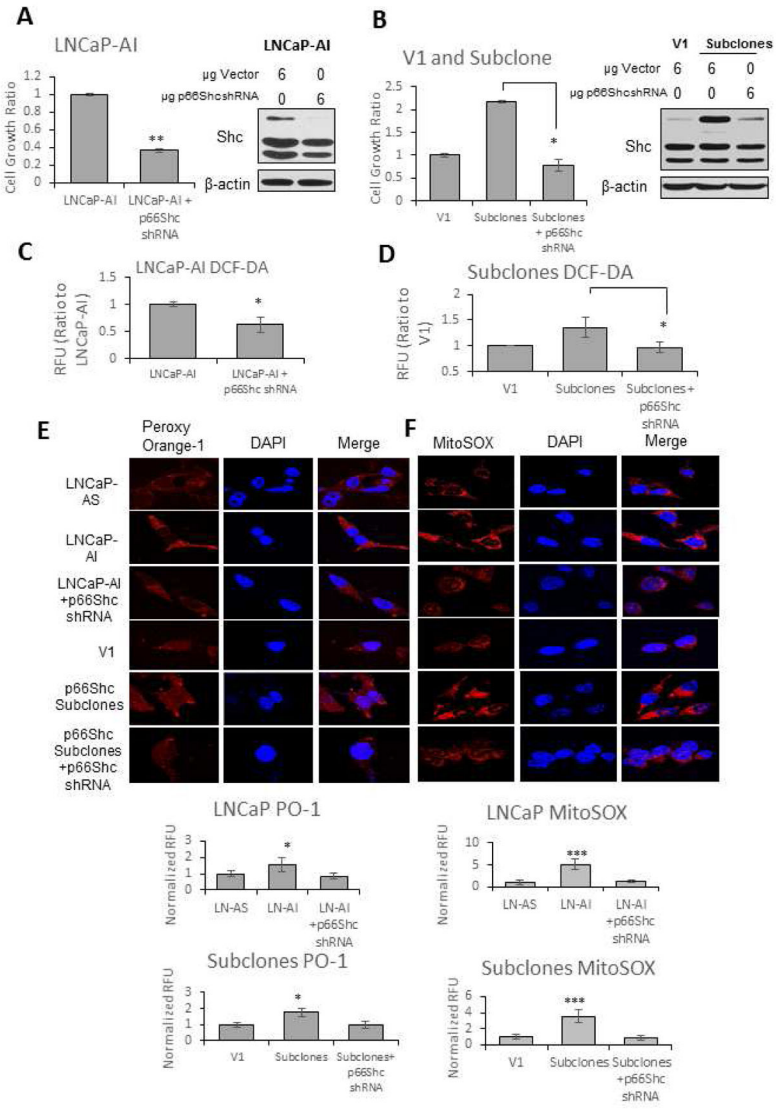

Figure 5. Cell Proliferation and Cellular Oxidative Environment in LNCaP-AS and LNCaP-AI Cells and p66Shc Subclones.

(A) LNCaP-AI and (B) p66Shc subclone cells were plated at 2×10^4 cells per well in 6-well plates for 48 hours. Cells were transfected with vector or p66Shc shRNA, then grown for an additional 72 hours before cells were harvested via trypsin. Cell viability was measured using Trypan blue exclusion dye. Results presented are mean ± SD. n=3×3. *p<0.05, **p<0.005, ***p<0.0005. Cells were then lysed to determine Shc protein levels via Western blot analysis to confirm proper transfection. β-actin protein level was used as a loading control.

(C) LNCaP-AI and (D) p66Shc subclone cells were plated at 2×10^5 cells per T25 flasks for 48 hours. Cells were transfected with vector or p66Shc shRNA, then grown for an additional 24 hours before cells were harvested via trypsin. Cells were stained with DCF-DA (20 μM) for 30 minutes in the dark and subjected to flow cytometry analysis. Results presented are mean ± SD. n=3.

LNCaP-AS and LNCaP-AI cells and p66Shc subclones with vector alone transfected V1 cells were plated at 5×10^4 cells per well in 12-well plates for 48 hours. Cells were transfected with vector or p66Shc shRNA, then grown for an additional 24 hours. (E) H_2O_2 was labeled with Peroxy Orange-1 fluorescence indicator for 1 hour before the reaction was quenched. (F) Mitochondrial $O_2^{\bullet -}$ levels were labeled with MitoSOX fluorescence indicator for 1 hour. DAPI was utilized to stain the nucleus. Fluorescence was visualized via a confocal microscope. Color adjustment was applied equally in all images shown. The data shown is a representative of three sets of independent experiments and similar results were obtained. Twenty cells were imaged for each treatment in each independent experiment. Results presented are mean ± SD. n=3. *$p<0.05$, **$p<0.005$.

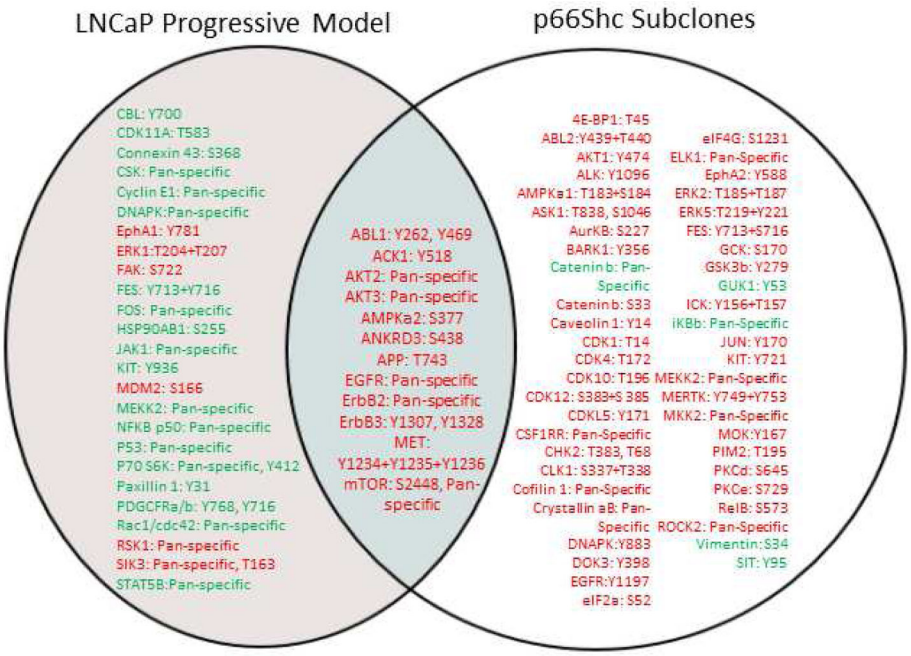

Figure 6. Phosphoprotein Microarray Analysis of LNCaP Cell Progression Model and p66Shc Subclones.

Total cell lysates of LNCaP-AS and LNCaP-AI cells or V1 control cells and equally mixed population of stable S31, S32, and S36 p66Shc subclones were analyzed via KAM-900P protein microarray by Kinexus. Results are presented in which red represents an increase and green a decrease in phosphoprotein or protein levels comparing the LNCaP-AI cells or p66Shc subclones to AS LNCaP or V1 cells, respectively. n=1×5.

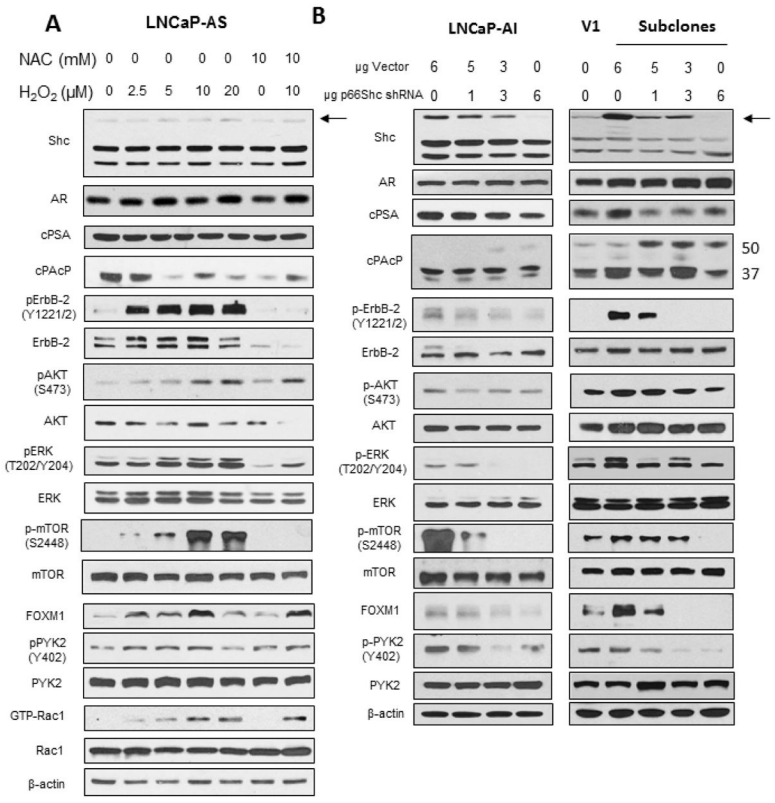

Figure 7. Oxidant Species/p66Shc Effect on Signaling Profile in LNCaP-AS Cells and p66Shc Subclones.

Immunoblot analysis of (A) LNCaP-AS cells upon treatment with H_2O_2 (10 μM) and/or NAC (10 mM) and (B) LNCaP-AI cells and p66Shc subclones upon knockdown of p66Shc. Cells were plated in T75 flasks at 1.5×10^4 cells per flask in regular steroid-containing medium for 72 hours, before being treated with H_2O_2 (0-20 μM) and/or NAC (10 mM) for 72 hours. Cells were harvested via scrapping and lysed. (A) Total cell lysates were analyzed for Shc, AR, cPSA, PAcP and FOXM1. Lysates were also analyzed for total and phosphorylated ErbB-2, AKT, ERK, mTOR, and PYK2 as well as total and GTP-Rac1. (B) Total cell lysates of LNCaP-AI and p66Shc subclone cells transfected with p66Shc shRNA were analyzed for Shc and FOXM1. Lysates were also analyzed for total and phosphorylated ErbB-2, AKT, ERK, mTOR and PYK2. β-actin protein level was used as a loading control. The data shown is a representative of three sets of independent experiments and similar results were obtained. n=3.

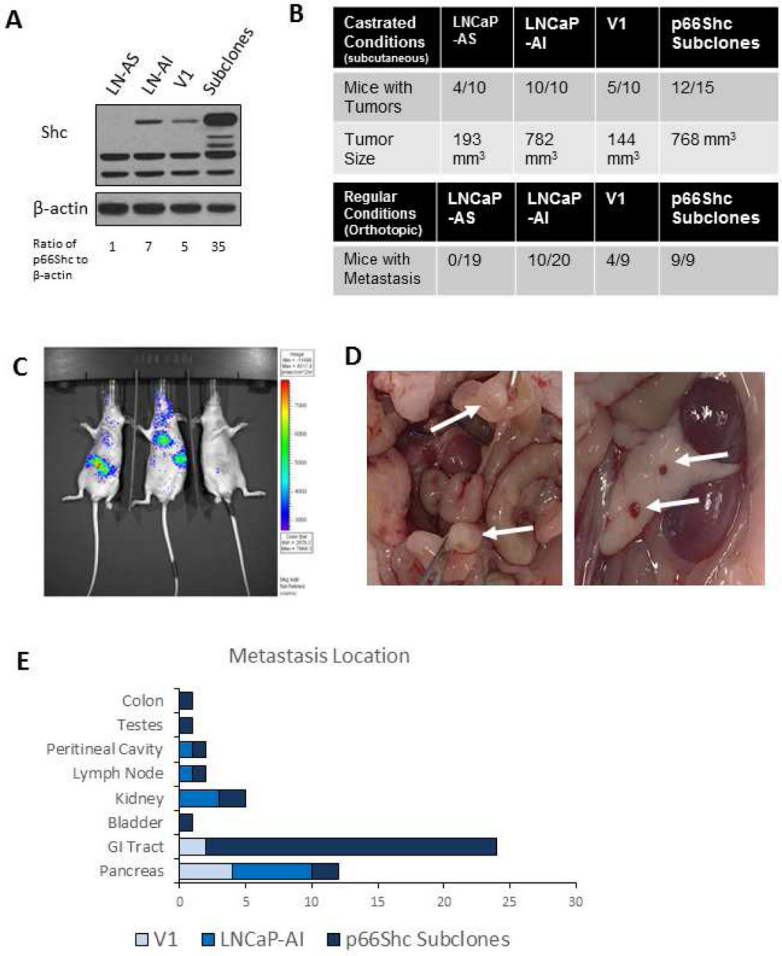

Castrated Conditions (subcutaneous)	LNCaP -AS	LNCaP -AI	V1	p66Shc Subclones
Mice with Tumors	4/10	10/10	5/10	12/15
Tumor Size	193 mm^3	782 mm^3	144 mm^3	768 mm^3
Regular Conditions (Orthotopic)	**LNCaP -AS**	**LNCaP -AI**	**V1**	**p66Shc Subclones**
Mice with Metastasis	0/19	10/20	4/9	9/9

Figure 8. ***In vivo*** **Models of LNCaP Cell Progression Model and p66Shc Subclones.**

(A) Western blot analysis of Shc in LNCaP-AS, LNCaP-AI, V1 and p66Shc subclone cells. β-actin protein level was used as a loading control.

(B-D) Orthotopic injection of 2×10^6 AS or AI LNCaP cells into male athymic nude mouse prostates or subcutaneous injection of 1×10^6 AS or AI LNCaP cells or V1 and p66Shc subclones into male (regular conditions) or female (castrated conditions) mice dorsal surface. Tumors were allowed to grow for 8 weeks before animals were sacrificed. (B) Mice with metastasis 7-8 weeks post orthotopic injection was recorded. (C) Imaging of LNCaP-AI-LUC tumors in mice 3 weeks post-implantation. (D) Photograph of p66Shc subclone tumor metastasis to the GI tract (left) and pancreas (right). (E) Locations of metastatic foci in mice implanted with LNCaP-AI and p66Shc subclones tumors.

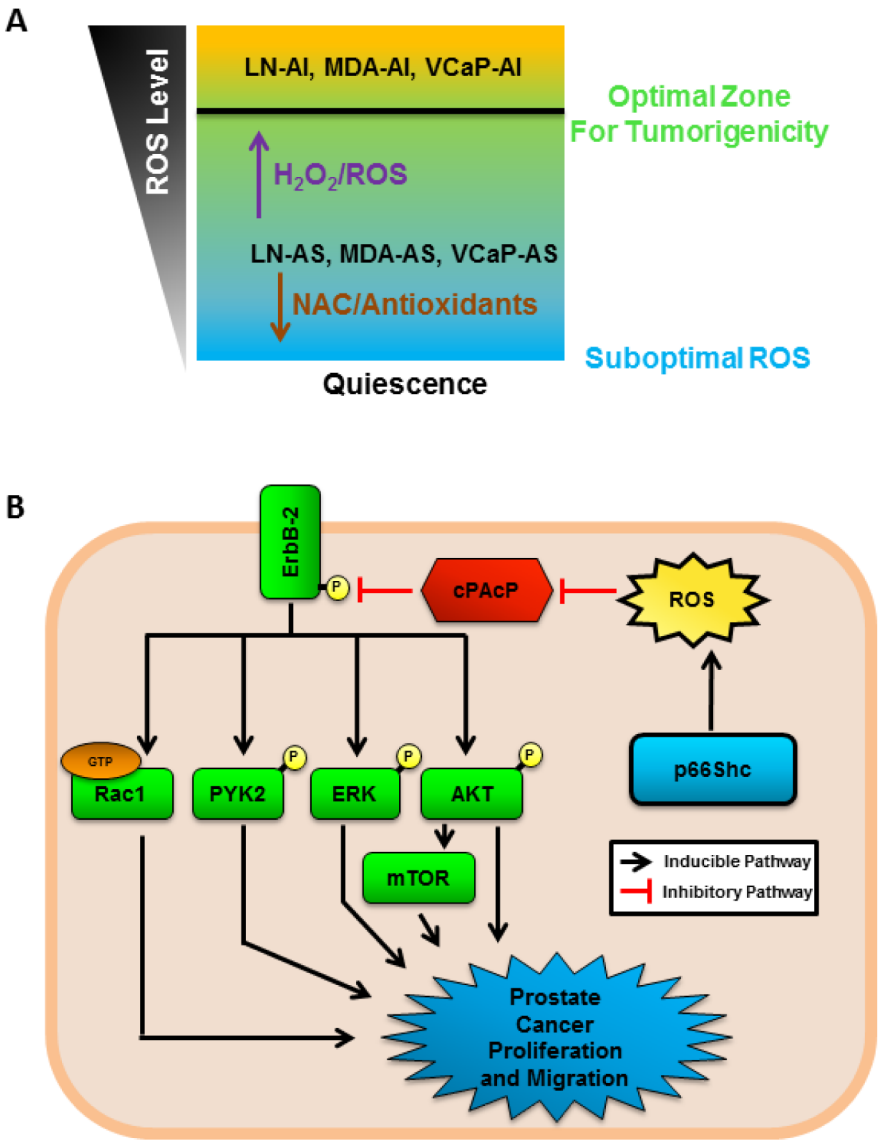

Figure 9. Dynamic Balance of ROS/Oxidant Species in PCa Progression.

(A) Diagram of the balance of ROS/oxidant species in PCa cells. PCa cells are documented to have higher levels of ROS than benign tissue. AS PCa cells have moderate levels of ROS, which can be reduced by NAC treatment or antioxidant enzymes to reduce tumorigenicity and induce quiescence. Increased ROS in AS PCa cells via H_2O_2 or pro-oxidants can promote PCa tumorigenicity and thus, more aggressive cancer and obtain the CR phenotype. (B) p66Shc protein has been demonstrated to enhance oxidant species production and is elevated in prostate cancer cells. Increased cellular oxidant species oxidize cellular prostatic acid phosphatase (cPAcP), preventing it from dephosphorylating ErbB-2. Phosphorylated ErbB-2 then activates downstream targets PI3K/AKT/mTOR, ERK, PYK2 and Rac1, all of which contribute to PCa cell proliferation and migration.